Constitutive phosphorylation of MDC1 physically links the MRE11–RAD50–NBS1 complex to damaged chromatin

Christoph Spycher,[1] Edward S. Miller,[3] Kelly Townsend,[3] Lucijana Pavic,[1] Nicholas A. Morrice,[4] Pavel Janscak,[2] Grant S. Stewart,[3] and Manuel Stucki[1]

[1]Institute of Veterinary Biochemistry and Molecular Biology and [2]Institute of Molecular Cancer Research, University of Zürich, 8057 Zürich, Switzerland
[3]Cancer Research UK Institute for Cancer Studies, Birmingham University, Birmingham B15 2TT, England, UK
[4]Medical Research Council Protein Phosphorylation Unit, School of Life Sciences, University of Dundee, Dundee DD1 5EH, Scotland, UK

The MRE11–RAD50–Nijmegen breakage syndrome 1 (NBS1 [MRN]) complex accumulates at sites of DNA double-strand breaks (DSBs) in microscopically discernible nuclear foci. Focus formation by the MRN complex is dependent on MDC1, a large nuclear protein that directly interacts with phosphorylated H2AX. In this study, we identified a region in MDC1 that is essential for the focal accumulation of the MRN complex at sites of DNA damage. This region contains multiple conserved acidic sequence motifs that are constitutively phosphorylated in vivo. We show that these motifs are efficiently phosphorylated by caseine kinase 2 (CK2) in vitro and directly interact with the N-terminal forkhead-associated domain of NBS1 in a phosphorylation-dependent manner. Mutation of these conserved motifs in MDC1 or depletion of CK2 by small interfering RNA disrupts the interaction between MDC1 and NBS1 and abrogates accumulation of the MRN complex at sites of DNA DSBs in vivo. Thus, our data reveal the mechanism by which MDC1 physically couples the MRN complex to damaged chromatin.

Introduction

Eukaryotic cells are equipped with sophisticated mechanisms to detect, signal the presence of, and repair DNA damage. Of particular importance are the pathways that deal with DNA double-strand breaks (DSBs): highly toxic lesions that, if unrepaired or repaired incorrectly, can cause cell death, mutations, and chromosomal translocations and can lead to diseases such as cancer. Cells react to DSBs by rapidly deploying a host of proteins to the damaged chromatin regions. Some of these factors engage in DNA repair, whereas others trigger a signaling pathway (called the DNA damage checkpoint) that provokes delays in cell cycle progression and coordinates the repair process; together, these events comprise the so-called DNA damage response (DDR; Zhou and Elledge, 2000).

Among the first proteins that accumulate at sites of DSBs in eukaryotic cells is the MRE11–RAD50–Nijmegen breakage syndrome 1 (NBS1 [MRN]) complex, a conserved and essential DDR factor that functions in a multitude of cellular processes involving DSBs, including DSB repair, checkpoint signaling, DNA replication, meiotic recombination, and induction of apoptosis (Stracker et al., 2004, 2007; Difilippantonio et al., 2007). The MRN complex consists of three subunits. The first is the structure-specific nuclease MRE11, which is most likely involved in nucleolytic processing of DNA ends to allow homologous recombination repair (Jazayeri et al., 2006), and the second is the ATPase and adenylate kinase subunit RAD50, which, together with MRE11, appears to facilitate tethering of DNA molecules to promote DSB repair (Costanzo et al., 2004; Bhaskara et al., 2007). The third subunit of the MRN complex, NBS1, does not exhibit any catalytic activities. Instead, its domain composition suggests that it belongs to the family of adaptor/mediator proteins of the DDR, a group of recently emerging factors that integrate, coordinate, and enhance the various cellular responses to DNA damage by promoting protein–protein interactions (D'Amours and Jackson, 2002). Consistent with this notion, NBS1 features both forkhead-associated (FHA) and BRCA1 C-terminal (BRCT) domains at its N terminus, which are protein interaction modules that specifically mediate the interaction with

Correspondence to Manuel Stucki: m.stucki@vetbio.uzh.ch

Abbreviations used in this paper: ATM, ataxia telangiectasia mutated; BRCT, BRCA1 C terminal; CK, caseine kinase; DDR, DNA damage response; DSB, double-strand break; FHA, forkhead associated; IR, ionizing radiation; MEF, mouse embryonic fibroblast; MR, MRE11 and RAD50; MRN, MRE11–RAD50–NBS1; NBS, Nijmegen breakage syndrome; PIKK, phosphoinositide-3-kinase–related protein kinase; PNK, polynucleotide kinase; pSDpT, phosphorylated SDT peptide; PST, Pro-Ser-Thr; SDT, Ser-Asp-Thr; TBB, tetrabromo-2-azabenzimidazole.

The online version of this article contains supplemental material.

The Journal of Cell Biology, Vol. 181, No. 2, April 21, 2008 227–240
http://www.jcb.org/cgi/doi/10.1083/jcb.200709008

phosphorylated proteins (Durocher and Jackson, 2002; Glover et al., 2004). Moreover, several NBS1 interaction partners have been described; most prominent among these is the ataxia telangiectasia mutated (ATM) kinase, the key upstream component of DSB signaling (Falck et al., 2005). Mutations in the *NBS1* gene leads to NBS in humans, and cells derived from NBS patients display a DSB repair and signaling deficiency, including radiosensitivity, chromosomal instability, and checkpoint defects (D'Amours and Jackson, 2002). Mouse models in which the native mouse *NBS1* allele was exchanged with hypomorphic mutant alleles recapitulate many features of NBS in the mouse, including developmental defects, chromosomal instability, and checkpoint deficiency (Difilippantonio et al., 2005, 2007).

Accumulation of the MRN complex at sites of DSBs is manifested by the formation of microscopically discernible subnuclear structures, so-called nuclear foci that represent large chromatin regions containing one or several unrepaired DSBs (Maser et al., 1997). The key regulator of nuclear foci formation in higher eukaryotes is the histone variant H2AX, an integral component of the nucleosome core structure that comprises 10–15% of total cellular H2A in higher organisms (Fernandez-Capetillo et al., 2004). H2AX is phosphorylated extensively on a conserved Ser residue at its C terminus in chromatin regions bearing DSBs, and this is mediated mainly by the ATM kinase, a member of the phosphoinositide-3-kinase–related protein kinase (PIKK) family (Burma et al., 2001).

Although it has been previously suggested that MRN accumulation at sites of DSBs occurs through interaction between the FHA/BRCT region of NBS1 and phosphorylated H2AX (γ-H2AX; Kobayashi et al., 2002), recent evidence suggests that the interaction between NBS1 and γ-H2AX is not direct but is mediated by MDC1, a large nuclear factor that interacts with the MRN complex and also features the criteria of a DDR mediator/adaptor protein, including the presence of FHA and BRCT domains (for review see Stucki and Jackson, 2004). First, it was shown that MDC1 exists in a complex with MRN in extracts of undamaged cells (Goldberg et al., 2003). This complex dissociates upon modification of the N-terminal FHA domain of NBS1, suggesting that the NBS1 FHA domain may be participating in the interaction between the two factors (Lukas et al., 2004). Second, MDC1 directly and specifically interacts with the phosphorylated H2AX C terminus through its tandem BRCT domains (Stucki et al., 2005). The x-ray structure of the MDC1–γ-H2AX complex suggests that the MDC1 BRCT domains are uniquely tailored to interact with the γ-H2AX chromatin mark (Stucki et al., 2005). Third, a phosphopeptide derived from the H2AX C terminus interacted with the MRN complex only in the presence of MDC1 (Lukas et al., 2004). Fourth, experimental disruption of the interaction between MDC1 and γ-H2AX (Stucki et al., 2005) or loss of MDC1 expression by genetic manipulation and/or siRNA-mediated depletion leads to a complete abrogation of MRN foci formation (Goldberg et al., 2003; Stewart et al., 2003; Lukas et al., 2004; Lou et al., 2006). Finally, mutations in the N-terminal FHA/BRCT region of NBS1 also interfere with MRN accumulation at sites of DSBs (Kobayashi et al., 2002; Zhao et al., 2002; Cerosaletti and Concannon, 2003; Lee et al., 2003; Horejsi et al., 2004).

MDC1 is composed of several distinct sequence domains. Besides an FHA domain at its N terminus and the γ-H2AX–interacting BRCT tandem domain at the C terminus, MDC1 also features a unique repeat region in the middle of the protein (Pro-Ser-Thr [PST] repeat) and contains several highly conserved putative PIKK target sites, some of which are phosphorylated in response to DNA damage in vivo (Matsuoka et al., 2007). In addition, MDC1 is also phosphorylated in the absence of DNA damage: several recent large-scale phosphorylation site screens of the human and mouse proteome revealed that MDC1 is constitutively phosphorylated on a significant number of Ser and Thr residues in vivo (Beausoleil et al., 2004; Olsen et al., 2006; Villen et al., 2007).

Although it is well established that MDC1 mediates the accumulation of many DDR factors in damaged chromatin regions (including the MRN complex, 53BP1, BRCA1, and ATM; Stucki and Jackson, 2006), it is still unclear how MDC1 mediates MRN recruitment. The observation that MDC1 exists in a complex with MRN in extracts from undamaged cells suggests that MDC1 may recruit MRN to γ-H2AX–containing chromatin in a simple "piggyback ride" mechanism whereby the physical interface between the two factors is made up by the NBS1 N-terminal FHA/BRCT region and by one or several phosphoepitopes on MDC1.

To put such a mechanism to the test, we set up an in vivo complementation system for MDC1 to search for a region in MDC1 that is responsible to mediate MRN foci formation. Through this approach, we identified a new region in MDC1 that is composed of several acidic repeats featuring a unique sequence motif, the Ser-Asp-Thr (SDT) motif. Furthermore, we provide evidence that these SDT repeats are constitutively phosphorylated by caseine kinase 2 (CK2) and that the phosphorylated form of these motifs constitute the phosphoepitope that the NBS1 FHA domain is binding to. These findings allow us to draw a model of the mechanism by which MDC1 physically links the MRN complex to damaged chromatin.

Results

An acidic region near the N terminus of MDC1 is essential for NBS1 foci formation

Efficient accumulation of the MRN complex in foci at sites of DSBs is critically dependent on MDC1 (Goldberg et al., 2003; Lukas et al., 2004). To determine the region of MDC1 that mediates MRN foci formation, we transfected MDC1$^{-/-}$ mouse embryonic fibroblasts (MEFs; Lou et al., 2006) with a series of N-terminal deletion mutants of mouse MDC1 and assessed MRN accumulation by indirect immunofluorescence using an antibody specific for mouse NBS1 (Celeste et al., 2003). Consistent with published data (Lou et al., 2006), MDC1$^{-/-}$ MEFs were completely defective for NBS1 accumulation (unpublished data), but transient transfection of these cells with HA-tagged full-length mouse MDC1 readily restored NBS1 foci formation in response to 5 Gy of ionizing radiation (IR; Fig. 1 B, WT). Deletion of 153 and 295 N-terminal amino acids of MDC1 did not result in any detectable reduction of NBS1 foci (Fig. 1 B, ΔN1 and ΔN2), but deletion of 452 and 645 amino acids led to a complete loss of NBS1 accumulation (Fig. 1 B, ΔN3 and ΔN4). This indicated that the region in MDC1 essential for mediating NBS1 accumulation is located somewhere between amino acids 295 and 452. Indeed, internal deletion of this 157–amino acid region completely abolished

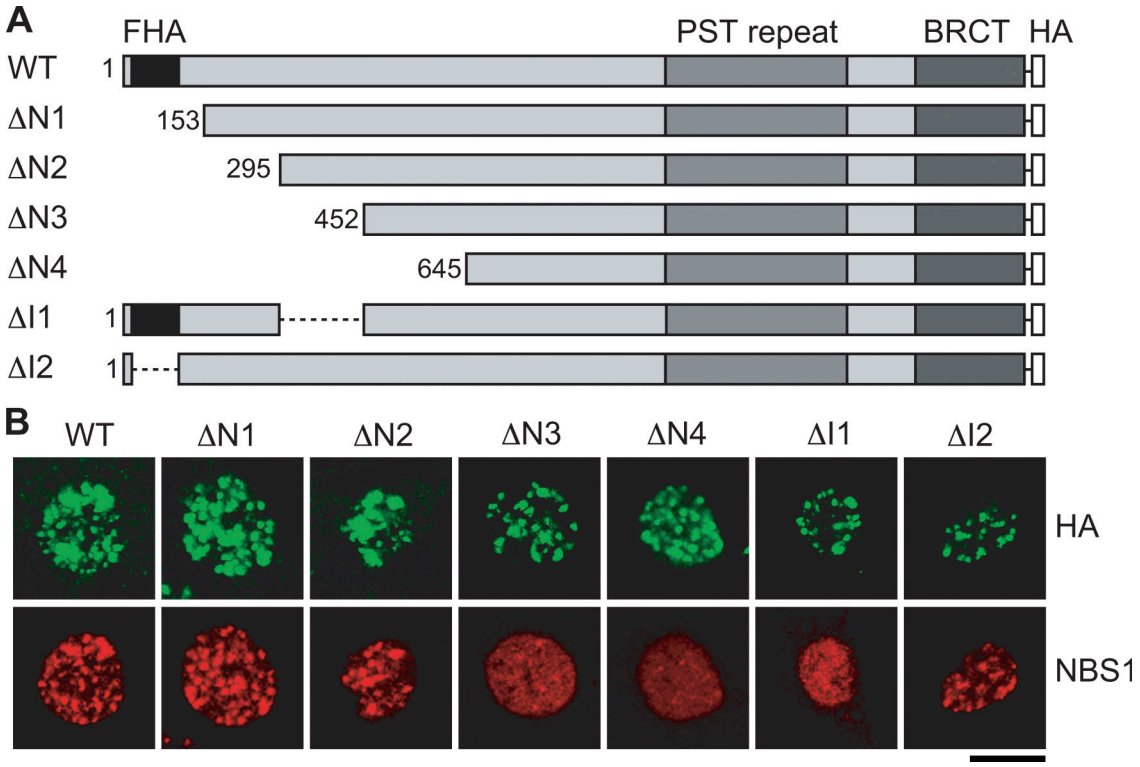

Figure 1. **An acidic domain near the N terminus of MDC1 is essential for NBS1 foci formation.** (A) Schematic representation of HA-tagged full-length mouse MDC1 and various deletion mutants. (B) MDC1$^{-/-}$ MEFs were transiently transfected with wild-type (WT) MDC1 and the individual deletion constructs. 48 h later, cells were irradiated, fixed with methanol, and stained with antibodies specific for HA and mouse NBS1. Nuclear foci were assessed by confocal microscopy. Bar, 10 µm.

the ability of MDC1 to mediate NBS1 foci formation (Fig. 1 B, ΔI1). Preliminary sequence analysis of this region revealed a significant abundance of acidic amino acids as compared with other regions of MDC1 (Fig. 2 A).

Interestingly, deletion of a region between amino acids 51 and 107 of mouse MDC1 (containing the FHA domain) did not have any effect on NBS1 accumulation (Fig. 1, ΔI2) even though overexpression of the FHA domain was reported to trigger a dominant-negative effect on NBS1 foci formation (Goldberg et al., 2003). In summary, these results suggest that an acidic region near the N terminus of MDC1 mediates MRN accumulation at sites of DSBs.

Phosphorylation-dependent interaction between the MDC1 N terminus and the MRN complex

To understand how the region identified by the systematic deletion analysis mediates MRN foci formation, we carefully analyzed the sequence between amino acids 295 and 452 of mouse MDC1. As mentioned in the previous section, this region of MDC1 is highly acidic with a calculated isoelectric point of 4.04. To detect conserved sequence motifs within this region, we compared the mouse sequence to MDC1 sequences from other vertebrate species (including human, dog, swine, and zebrafish). This analysis revealed several conserved patches of 8–10 amino acids interspersed with less conserved regions of variable length (Fig. 2 A; patches are highlighted by horizontal bars). The conserved patches feature a repeated sequence motif: Ser and Thr residues are embedded in an acidic sequence environment. A single amino acid (typically Asp) sits in between the highly conserved Ser and Thr residues. Thus, we hereafter refer to this motif as the SDT motif. The motif also contains two to three consecutive acidic amino acids (usually Glu) that are five residues C terminal to the initial Ser. Mammalian MDC1 contains a total of six SDT motifs (Fig. S1, available at http://www.jcb.org/cgi/content/full/jcb.200709008/DC1): five are located within the region of MDC1, whose deletion abrogates MRN foci (Fig. 2 A), and one is located ∼80 amino acids N terminal to this region (not depicted). Zebrafish MDC1 features a total of eight SDT motifs, and even honey bee MDC1 (the only clear nonvertebrate MDC1 orthologue identified to date) comprises a very similar motif (Fig. S1), indicating that the SDT motif is conserved in all known MDC1 orthologues.

In untreated mammalian cells, MDC1 is a phosphoprotein that becomes rapidly hyperphosphorylated in response to DNA damage in a PIKK-dependent manner (Goldberg et al., 2003; Stewart et al., 2003). A large number of constitutive and DNA damage–induced phosphorylation sites have recently been identified in MDC1 by means of several large-scale mass spectrometry screens of the human and mouse proteome (Beausoleil et al., 2004; Olsen et al., 2006; Matsuoka et al., 2007; Villen et al., 2007). Interestingly, many of the constitutive phosphorylation sites of MDC1 are located within the SDT motifs (Fig. 2 A). In summary, it appears that in human cells, a population of MDC1 molecules is phosphorylated on any Ser and Thr residue in at least four of the six SDT motifs in vivo (Beausoleil et al., 2004; Olsen et al., 2006). In addition, mouse MDC1 appears to be phosphorylated in at least one SDT motif (Villen et al., 2007).

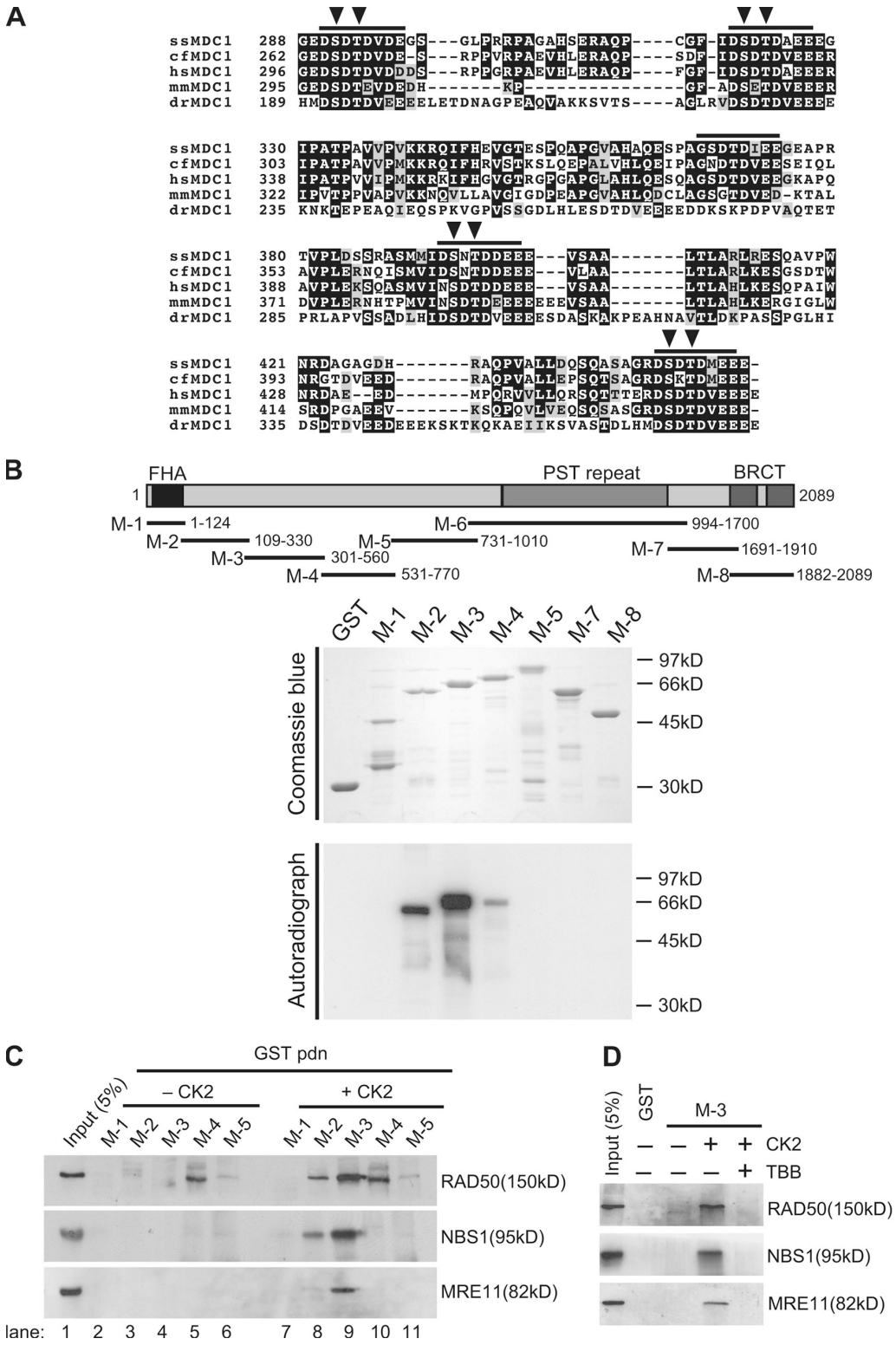

Figure 2. **Phosphorylation-dependent interaction between the MDC1 N terminus and the MRN complex.** (A) Sequence alignment of the region in MDC1 that is essential for MRN foci. The conserved acidic motifs are highlighted by horizontal bars. Phosphorylated residues identified by in vivo phosphorylation site mapping are highlighted by arrowheads (Beausoleil et al., 2004; Olsen et al., 2006; Villen et al., 2007). (B, top) Representation of human MDC1 and the overlapping GST fragments. (bottom) Two fragments at the N terminus of MDC1 are phosphorylated by CK2 in vitro. Purified GST-MDC1 fragments were incubated with purified recombinant CK2 in the presence of radioactive ATP. Proteins were separated by SDS-PAGE, and dried gels were subjected to autoradiography. A Coomassie blue–stained gel of the purified GST fragments is shown on top of the autoradiograph. Note that fragment M-6 (PST repeat region) was not expressed in bacteria. (C) Purified GST-MDC1 fragments (M-1–5) were preincubated with and without recombinant CK2 in the presence of ATP. (D) Purified GST-MDC1 fragment M-3 was preincubated with CK2 either in the presence or absence of the CK2 inhibitor TBB. (C and D) The fragments were then used to pull down proteins from HeLa nuclear extract. Bound proteins were separated on SDS-polyacrylamide gels followed by immunoblotting. The blots were probed with antibodies against RAD50, NBS1, and MRE11.

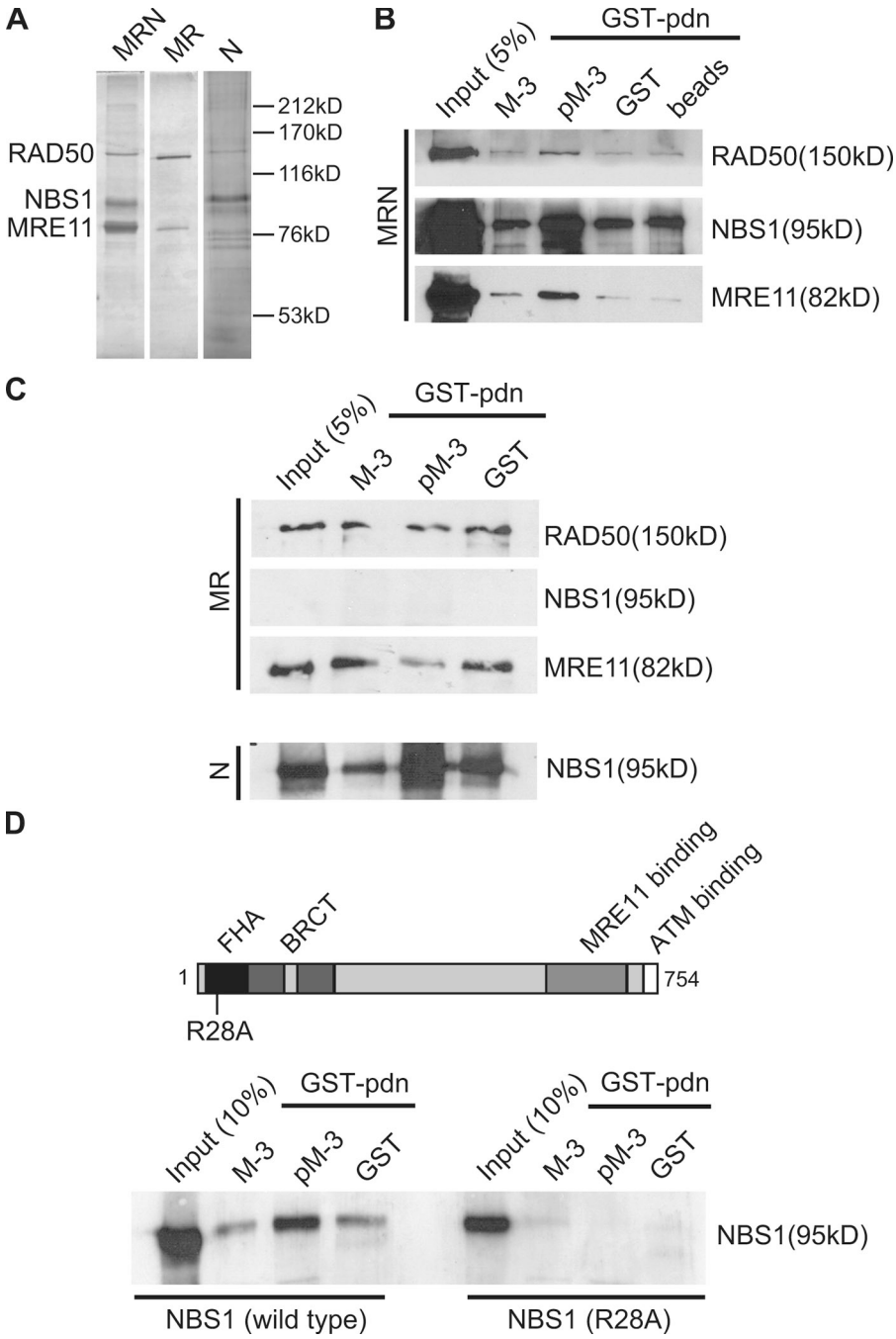

Figure 3. **Direct interaction between the phosphorylated MDC1 N terminus and the MRN complex is mediated by the NBS1 FHA domain.** (A) MRN proteins were purified as described in Materials and methods. Proteins were separated on SDS-polyacrylamide gels and stained with silver. MR, MRE11–RAD50 subcomplex; N, partially purified NBS1. (B and C) Purified GST-MDC1 fragment M-3 comprising part of the SDT region was preincubated with CK2 and ATP. The fragment was incubated with purified MRN complex (B), purified MR subcomplex (C, top), and partially purified NBS1 (C, bottom) followed by GST pull-down analysis. Bound proteins were separated on SDS-polyacrylamide gels followed by immunoblotting. The blots were probed with antibodies against RAD50, NBS1, and MRE11. (D, top) Schematic representation of NBS1 with its functional domains. (bottom) Purified GST-MDC1 fragment M-3 was preincubated with CK2 and ATP. The fragment was incubated with purified MRN complex where the NBS1 subunit was either wild type or contained a point mutation in the FHA domain (R28A). Bound proteins were separated on SDS-polyacrylamide gels followed by immunoblotting. The blots were probed with a polyclonal antibody against NBS1.

The acidic nature of the SDT motif suggests that it may be targeted by acidophilic kinases such as CK1 and 2. Indeed, analysis of the MDC1 SDT domain by Scansite (Yaffe et al., 2001) revealed that the sequence encompassing the Ser and Thr residues within the SDT motifs conform to consensus CK2 phosphorylation sites. To test whether CK2 would specifically phosphorylate MDC1 in the SDT region, we generated eight overlapping random fragments of the human MDC1 cDNA and expressed them in *Escherichia coli* as GST fusion proteins. Seven fragments were expressed well and were purified (Fig. 2 B, top), whereas one fragment (M-6) comprising the MDC1 PST repeat region was not expressed in bacteria. The purified fragments were subjected to an in vitro kinase assay using recombinant CK2. CK2 efficiently phosphorylated fragment M-2 (amino acids 109–330) and M-3 (amino acids 301–560) but none of the other five fragments. Fragment M-2 contains two SDT motifs, and fragment M-3 contains the other four SDT motifs.

MDC1 exists in a complex with MRN in extracts derived from undamaged cells, indicating that these proteins interact constitutively (Fig. S2, available at http://www.jcb.org/cgi/content/full/jcb.200709008/DC1). However, the mechanism of this interaction has not yet been elucidated. Significantly, GST pull-down analysis with our GST-MDC1 fragments revealed that fragment M-2 and M-3 only pulled down significant quantities of the MRN complex from HeLa nuclear extract when preincubated with recombinant CK2 and ATP (Fig. 2 C, compare lanes

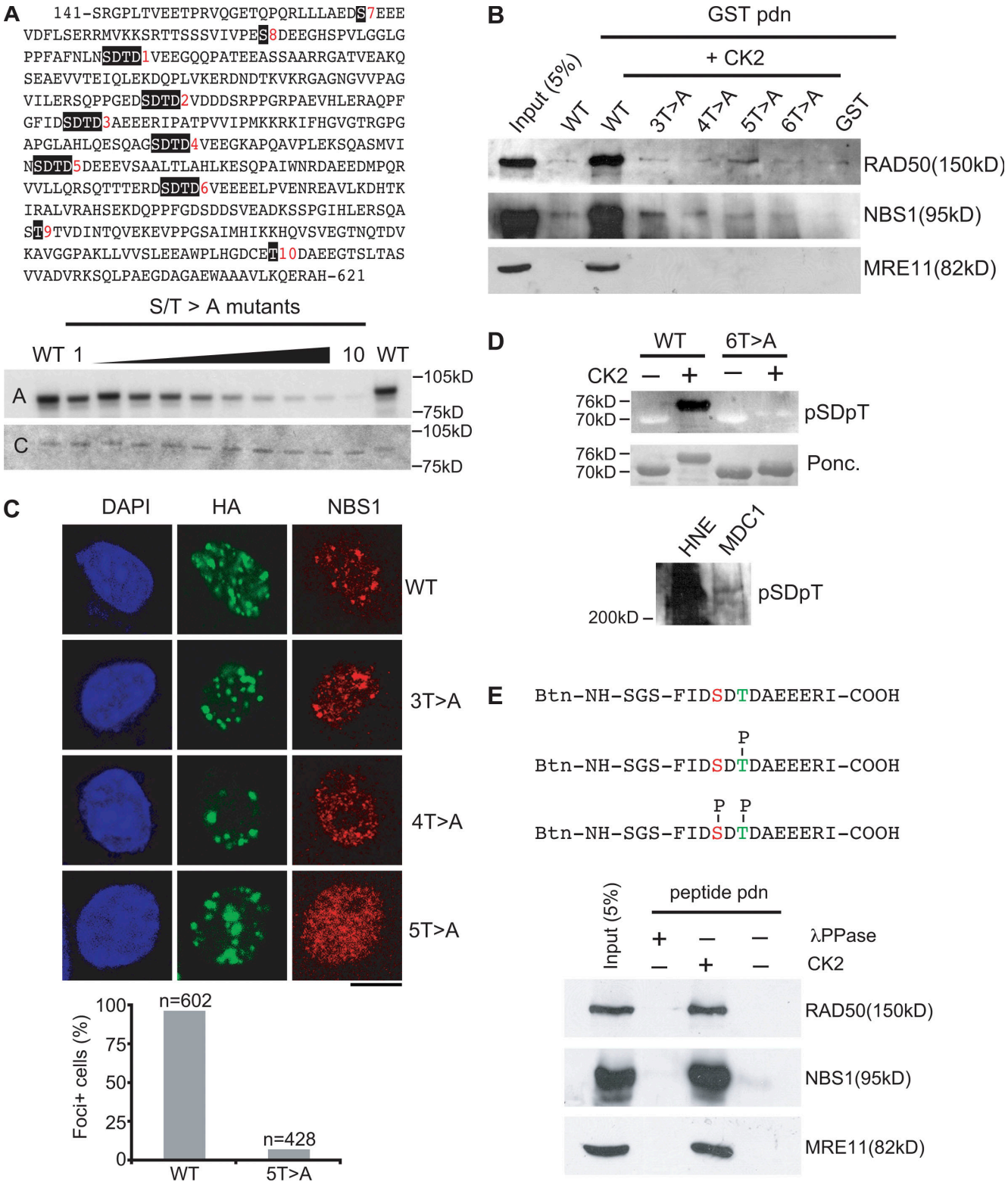

Figure 4. **A repeated phosphorylated motif in MDC1 mediates the interaction between MDC1 and NBS1.** (A) In vitro mapping of the CK2 phosphorylation sites in MDC1. (top) Sequence of the human MDC1 fragment comprising the conserved CK2 consensus sites (highlighted in black). The CK2 consensus sites are numbered from 1 to 10. (bottom) All of the putative CK2 phosphoacceptor Ser and Thr residues in the above MDC1 fragment (amino acids 141–621) were mutated to Ala, and the mutants were expressed as GST fusion proteins in *E. coli*. The GST fragments were incubated with purified recombinant CK2 in the presence of radioactive ATP. Proteins were separated by SDS-PAGE, and dried gels were subjected to autoradiography. A, autoradiograph; C, Coomassie blue–stained gel. (B) The SDT repeats are essential for the interaction between MDC1 and NBS1 in vitro. Several SDT motifs in a fragment derived from mouse MDC1 (amino acids 221–456) were mutated to SDA (3T>A: T362A, T387A, and T444A; 4T>A: T315A, T362A, T387A, and T444A; 5T>A: T300A, T315A, T362A, T387A, and T444A; 6T>A: T222A, T300A, T315A, T362A, T387A, and T444A) and were expressed as GST fusion proteins in *E. coli*. The purified fragments were preincubated with recombinant CK2 in the presence of ATP. The fragments were then used to pull down proteins from HeLa nuclear extract. Bound proteins were separated on SDS-polyacrylamide gels followed by immunoblotting. The blots were

Table I. **Tryptic MDC1 phosphopeptides**

MDC1 tryptic peptide	CK2 phosphorylation site
162-LLLAEDpSEEEVDFLSER-179	pS168
186-TTSSSVIVPESDEEGHSPVLGGLGPPFAFNLN(pSDpT)DVEEGQQPATEEASSAAR-238	$+2PO_4$
247-QSEAEVVTEIQLEKDQPLVK-266	NA
292-SQPPGEDpSDpTDVDDDSRPPGRPAEVHLERAQPFGFIDpSDpTDAEEERIPATPVVIPMK-348	pS299, pT301, pS329, pT331
361-PGAPGLAHLQESQAGpSDpTDVEEGKAPQAVPLEKSQASMVINpSDpTDDEEEVSAALTLAHLK-420	pS376, pT378, pS402, pT404
445-SQTTTERDpSDpTDVEEEELPVENR-467	pS453, pT455

NA, not applicable.

3 and 4 with lanes 8 and 9; note that the bands in lanes 5 and 10 in the top panel result from a cross-reactivity of the RAD50 antibody with a contaminating bacterial protein in the GST–M-4 fraction). In the absence of CK2, no interaction could be observed under these conditions (Fig. 2 C, lanes 2–6). In the presence of the specific CK2 inhibitor tetrabromo-2-azabenzimidazole (TBB), recombinant CK2 did not transform fragment M-3 into a form capable of pulling down the MRN complex from HeLa nuclear extract, indicating that CK2 activity is required for this process (Fig. 2 D). Together, these data suggest that the phosphorylated N-terminal region in MDC1 mediates the interaction with the MRN complex in vitro.

Direct interaction between the phosphorylated MDC1 N terminus and the MRN complex is mediated by the NBS1 FHA domain

To determine whether the MRN complex interacts directly with the phosphorylated MDC1 N terminus, we coexpressed all three MRN subunits and a subcomplex consisting of MRE11 and RAD50 (MR) in Sf9 cells by means of recombinant baculovirus infection followed by purification of the recombinant proteins to near homogeneity (Fig. 3 A, MRN and MR). We also isolated partially purified NBS1 alone (Fig. 3 A, N). Interaction studies with purified recombinant MRN, MR, and NBS1 were complicated by the fact that these proteins exhibited a significant unspecific binding activity toward the glutathione–Sepharose beads used in this analysis (Fig. 3 B, beads alone). Nevertheless, we consistently observed a significant enrichment of purified MRN and partially purified NBS1 when we used CK2-phosphorylated fragment M-3 in the pull-down assay (Fig. 3, B and C; bottom). Untreated M-3 or GST alone did not result in such enrichment. Similarly, neither phosphorylated nor unphosphorylated M-3 was capable of efficiently binding to MRE11/RAD50 in the absence of NBS1 (Fig. 3 C, top). In summary, these results indicate that the NBS1 subunit of the MRN complex directly associates with the phosphorylated M-3 fragment of MDC1 and mediates the interaction between MDC1 and the MRN complex.

NBS1 features two well-established phosphopeptide recognition modules at its N terminus: an FHA domain and a tandem BRCT domain (Fig. 3 D, top). It was previously shown that introduction of a point mutation in the FHA domain that changes a conserved Arg residue to Ala (R28A) disrupted the interaction between MDC1 and the MRN complex in vitro (Lukas et al., 2004) and abolished MRN accumulation at sites of DSBs in vivo (Cerosaletti and Concannon, 2003; Lee et al., 2003; Horejsi et al., 2004; Lukas et al., 2004). Thus, we isolated the MRN complex harboring the same mutation in NBS1 from baculovirus-infected Sf9 cells and compared its binding activity toward the phosphorylated M-3 fragment to the wild-type complex. Significantly, although the wild-type NBS1 readily interacted with phosphorylated M-3, no interaction was detected with the R28A mutant (Fig. 3 D). This indicates that an intact NBS1 FHA domain is essential for the interaction between the phosphorylated N-terminal region of MDC1 and the MRN complex.

A repeated phosphorylated motif in MDC1 mediates the interaction between MDC1 and NBS1

To map the phosphorylation sites within fragments M-2 and M-3 of MDC1, we isolated a new GST fragment comprising amino acids 141–621 of human MDC1 (M-SDT). The purified fragment was phosphorylated in vitro by recombinant CK2 followed by digestion with trypsin. The tryptic peptides were then analyzed by mass spectrometry. Thus, several phosphorylation sites were mapped (Table I), most notably all six of the conserved SDT motifs that were targeted by CK2 on both Ser and Thr residues. Next, all of the putative CK2 target Ser and Thr residues in the M-SDT fragment were mutated to Ala and expressed in *E. coli* (Fig. 4 A, top; the SDT motifs and other putative CK2 target sites are highlighted in black and numbered from 1–10). The purified mutants were subjected to in vitro phosphorylation by re-

probed with antibodies against RAD50, NBS1, and MRE11. (C) Mutation of a subset of the conserved SDT motifs abrogates NBS1 foci formation. (top) MDC1$^{-/-}$ MEFs were transiently transfected with various forms of HA-tagged full-length mouse MDC1, including wild-type (WT) and SDT-deficient (3T>A: T362A, T387A, and T444A; 4T>A: T315A, T362A, T387A, and T444A; 5T>A: T300A, T315A, T362A, T387A, and T444A) variants. 48 h later, cells were irradiated, fixed with methanol, and stained with antibodies against HA and mouse NBS1. (bottom) HA-positive cells were scored for NBS1 foci in wild-type and 5T>A-transfected populations (results were consistent in two independent datasets). (D) The SDT in MDC1 is phosphorylated in vivo. (top) A phosphospecific antibody raised against a doubly phosphorylated SDT peptide (pSDpT) was tested on CK2-phosphorylated GST-SDT. WT, mouse MDC1 (amino acids 221–456); 6T>A, all six SDT motifs were mutated to SDA. (bottom) Immunoblot analysis of phosphorylated MDC1 isolated from HeLa nuclear extract by a H2AX phosphopeptide using the pSDpT phosphospecific antibody. (E) A synthetic biotinylated peptide comprised of the SDT sequence motif and phosphorylated on the Thr residue was either left untreated or was preincubated with λ−PPase and CK2, respectively. (top) This leads to the three indicated products: unphosphorylated peptide, singly phosphorylated peptide (Thr), and doubly phosphorylated peptide (Ser and Thr). The peptides were then used to pull down proteins from HeLa nuclear extract. Proteins were detected as in B. Bar, 10 μm.

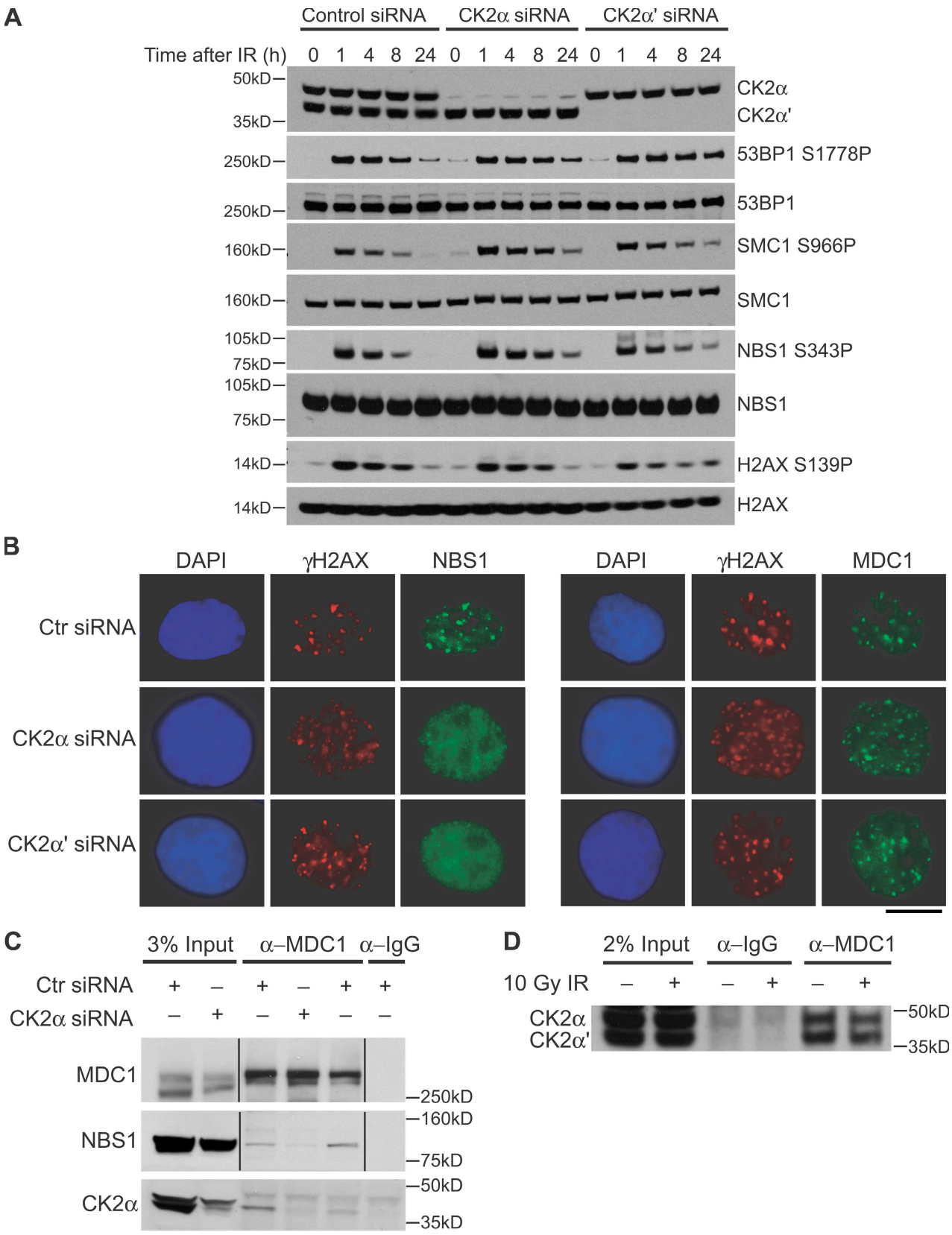

Figure 5. **CK2 is essential for the interaction between MDC1 and NBS1 and for the accumulation of NBS1 at sites of DSBs in vivo.** (A) Down-regulation of CK2α and CK2α′ by siRNA triggers a prolonged DDR. 72 h after transfection with siRNA duplexes, cells were irradiated and harvested at the indicated time points. Extracts were prepared and resolved by SDS-PAGE followed by immunoblotting. The blots were probed with the indicated antibodies. (B) Down-regulation of CK2α and CK2α′ by siRNA abrogates NBS1 accumulation at sites of DSBs. 72 h after transfection with siRNA duplexes, cells were irradiated, fixed with methanol, and stained with antibodies against γ-H2AX and NBS1. (C) Down-regulation of CK2α by siRNA disrupts the interaction between MDC1 and NBS1 in vivo. 72 h after transfection with siRNA duplexes, cells were lysed, and immunoprecipitation was performed using the

combinant CK2, and radioactive phosphate incorporation was measured by autoradiography (Fig. 4 A). This analysis revealed that all of the SDT motifs and other putative CK2 target sites were efficiently phosphorylated in vitro.

To test whether the highly conserved SDT repeats were necessary for the interaction with the MRN complex, we changed the conserved Thr residues to Ala within several SDT motifs and phosphorylated the isolated GST fusion proteins by CK2 in vitro. Significantly, GST pull-down analysis with the mutant fragments revealed that only the phosphorylated wild type was capable of pulling down significant quantities of the MRN complex from HeLa nuclear extract, whereas alteration of the three C-terminal SDT motifs (Fig. 4 A, 4–6) already reduced the interaction to almost background level (Fig. 4 B).

To test whether the SDT repeats of MDC1 mediate NBS1 accumulation at sites of DSBs in vivo, we introduced the same SDT mutations as before (Fig. 4 B) in the tagged full-length mouse MDC1 cDNA followed by transient transfection of MDC1$^{-/-}$ MEFs with those mutants and assessment of MDC1 and NBS1 foci formation by indirect immunofluorescence. Surprisingly, alteration of the last three C-terminal SDT motifs (Fig. 4 A, 4–6) did not trigger any significant reduction in NBS1 foci formation (Fig. 4 C, 3T>A) even though the corresponding GST fusion protein only weakly interacted with the MRN complex in vitro (Fig. 4 B, 3T>A). However, mutation of four SDT motifs (Fig. 4 A, 3–6) led to a detectable reduction in NBS1 accumulation even though small NBS1 foci were still detectable in a subset of the transfected cells (Fig. 4 C, 4T>A). Altering five of the six SDT motifs (Fig. 4 A, 2–6) completely abrogated NBS1 foci formation in all MDC1-positive cells (Fig. 4 C, 5T>A). Significantly, although the 5T>A mutant was unable to mediate NBS1 focal accumulation in response to IR, it still localizes to foci itself, indicating that an intact SDT region is not required for MDC1–γ-H2AX interaction.

Collectively, these results show that the SDT motifs are essential for the interaction between MDC1 and the MRN complex in vitro and for NBS1 accumulation at sites of DSBs in vivo, suggesting that the SDT motif may define a novel phosphospecific MRN-interacting element within MDC1. To test this directly, we first sought to ascertain that the SDT motifs of MDC1 are constitutively phosphorylated in vivo. To this end, we generated two phosphospecific antibodies against doubly phosphorylated SDT peptides (pSDpTs) derived from the human SDT repeat region (see Materials and methods for details). These antibodies were affinity purified and tested against the purified CK2-phosphorylated GST-SDT fragment and its 6T>A mutated derivative. Although one of the two antibodies did not recognize the CK2-phosphorylated GST-SDT fragment (not depicted), the other antibody specifically recognized GST-SDT only when it was preincubated with CK2 and ATP (Fig. 4 D, top). Significantly, the 6T>A mutant was not recognized at all by this antibody, indicating that it is specific for doubly phosphorylated SDT repeats. We next used this antibody to detect MDC1 in extracts from undamaged and irradiated mammalian cells. Unfortunately, the pSDpT antibody unspecifically cross-reacted with many proteins in whole cell and nuclear extracts, and, thus, we were unable to assess the MDC1 phosphorylation status in crude cell extracts (Fig. 4 D, bottom; first lane). However, MDC1 can be isolated along with the MRN complex from HeLa nuclear extract to near homogeneity by a phosphopeptide pull-down strategy using a phosphopeptide derived from the H2AX C terminus (Fig. S2; Stucki et al., 2005). When we probed the isolated MDC1–MRN complex with the pSDpT antibody, we observed two bands at the position where MDC1 runs on SDS gels, indicating that it is indeed phosphorylated on at least a subset of the SDT motifs in vivo (Fig. 4 D, bottom; second lane).

To clarify whether the MRN complex interacts with a single doubly phosphorylated SDT motif, we designed a biotinylated synthetic phosphopeptide comprising the sequence of one of the SDT motifs (Fig. 4 A, 3), which was phosphorylated on the Thr residue. This peptide was either left untreated or was treated with λ phosphatase and CK2. Mass spectrometry and in vitro CK2 assays revealed that such treatment resulted in singly phosphorylated SDpT peptide, unphosphorylated SDT peptide, and doubly phosphorylated pSDpT peptide (Fig. 4 E, top; and not depicted). Significantly, only the doubly phosphorylated peptide, in which both Ser and Thr residues are being phosphorylated, retrieved the MRN complex from HeLa nuclear extract (Fig. 4 E). Collectively, these results suggest that doubly phosphorylated SDT motifs interact with MRN and determine MRN accumulation in vivo.

CK2 is essential for the interaction between MDC1 and NBS1 and for the accumulation of NBS1 at sites of DSBs in vivo

Because the SDT repeats are efficiently targeted by CK2 in vitro (Fig. 4), we next sought to investigate whether CK2 activity was required for NBS1 accumulation at sites of DSBs in vivo. Several commercial small-molecule CK2 inhibitors are available, and two of them were tested on human and mouse cells (TBB and DMAT). Surprisingly, neither of the two inhibitors triggered a detectable reduction in NBS1 foci formation in cultured human and mouse cells (unpublished data). Thus, we speculated that there may either exist additional acidophilic kinases that are capable of efficiently phosphorylating the SDT repeats in MDC1 or that the inhibitors are not potent enough to completely eliminate SDT phosphorylation in our experimental settings.

To test the latter possibility, we took an siRNA approach to down-regulate the two catalytic subunits of CK2 (CK2α and CK2α′) in U2OS cells. 72 h after siRNA transfection, CK2α and CK2α′ expression reached background levels (Fig. 5 A). At the same time, we observed massive cell death and severe mitotic defects, corroborating the essential role of CK2 in the cellular metabolism and life cycle. Interestingly, we also

indicated antibodies. Proteins were separated by SDS-PAGE followed by immunoblotting. The blots were probed with antibodies against MDC1, NBS1, and CK2α. Black lines indicate that intervening lanes have been spliced out. (D) MDC1 is associated with CK2 in vivo. HeLa cell extracts were used to immunoprecipitate proteins with the indicated antibodies. The immunocomplexes were separated by SDS-PAGE followed by immunoblotting. The blot was probed with antibodies against CK2α and CK2α′. Bar, 10 μm.

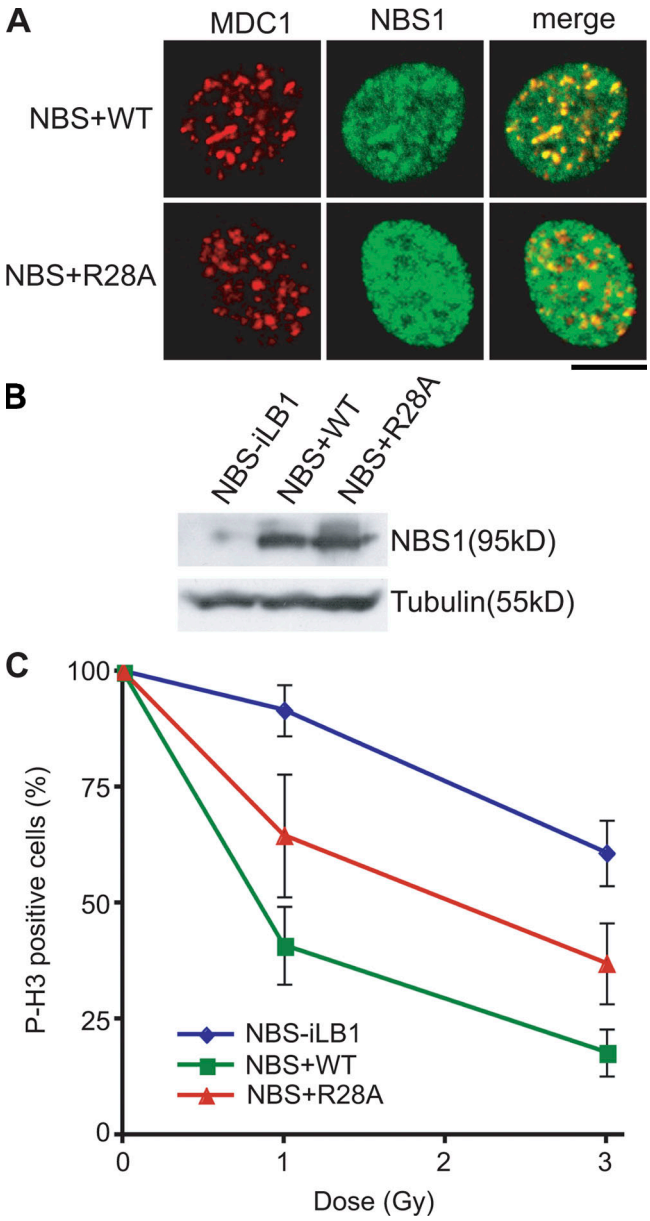

Figure 6. **Disruption of the MDC1–NBS1 interaction triggers a partial G2/M checkpoint defect.** (A) NBS-iLB1 fibroblasts and NBS-iLB1 fibroblasts stably transduced with wild-type NBS1 and R28A mutant NBS1 were irradiated, fixed with methanol, and stained with antibodies against MDC1 and NBS1. (B) Whole cell extracts of NBS-iLB1 fibroblasts and NBS-iLB1 fibroblasts stably transduced with wild-type (WT) NBS1 and R28A mutant NBS1 were resolved by SDS-PAGE followed by immunoblotting. The blot was probed with antibodies against NBS1 and tubulin. (C) NBS-iLB1 fibroblasts and NBS-iLB1 fibroblasts stably transduced with wild-type NBS1 and R28A mutant NBS1 were left untreated or irradiated with 1 Gy and 3 Gy, respectively. Cells were harvested 1 h after irradiation, fixed with methanol, and stained with an antibody against phosphorylated H3 (P-H3) and propidium iodine. The percentage of phosphorylated H3–positive cells was determined by FACS analysis. Error bars represent SD. Bar, 10 μm.

observed a prolonged phosphorylation of ATM substrates in response to IR (Fig. 5 A), suggesting that down-regulation of CK2 by siRNA may cause a repair defect.

Significantly, down-regulation of either CK2α or CK2α′ led to a marked defect in NBS1 foci formation in response to IR (Fig. 5 B, left). At the same time, MDC1 accumulation at sites of DSBs was not significantly reduced (Fig. 5 B, right) even though the foci appeared smaller as compared with the foci in control siRNA-treated cells. This indicates that CK2 is essential for the accumulation of NBS1 at sites of DSBs, whereas it is dispensable for the interaction between MDC1 and γ-H2AX.

Next, we tested whether CK2 was required for the constitutive interaction between MDC1 and NBS1. To this end, MDC1 antibodies were used to coimmunoprecipitate NBS1 from extracts derived from siRNA-treated human cells. No NBS1 coimmunoprecipitated with MDC1 from cells that were transfected with CK2α siRNA, whereas a small but significant amount of NBS1 coimmunoprecipitated with MDC1 from cell extracts that were prepared from control siRNA-transfected cells (Fig. 5 C). The membrane was also probed with an antibody against CK2α to monitor the efficiency of CK2α depletion (Fig. 5 C, bottom; note that CK2α corresponds to the faster migrating band). Interestingly, we noticed that CK2α also coimmunoprecipitated with MDC1 (Fig. 5 C, bottom; third and fifth lanes), indicating that CK2 may exist in a complex with MDC1 in vivo. Indeed, antibodies raised against MDC1 efficiently coimmunoprecipitated both CK2α and CK2α′ from HeLa cell extracts (Fig. 5 D). Notably, the interaction does not change upon the introduction of DNA damage by IR (Fig. 5 D, compare the last two lanes), indicating that it is constitutive and not induced by DNA damage.

Collectively, these data reveal that CK2 is essential for NBS1 foci formation and for the interaction between MDC1 and NBS1. In addition, CK2 exists in a complex with MDC1 and, thus, may be the primary kinase to target the SDT repeats in vivo.

Disruption of the MDC1–NBS1 interaction triggers a partial G2/M checkpoint defect

As shown in Fig. 3 D, the R28A mutation in the NBS1 FHA domain triggers a severe defect in the association of NBS1 with the CK2-phosphorylated MDC1 SDT region in vitro (Fig. 3 D). Consistent with previous studies (Cerosaletti and Concannon, 2003; Lee et al., 2003; Horejsi et al., 2004), we also observed that this mutant is unable to accumulate in foci in stably transduced NBS fibroblasts, whereas MDC1 accumulation is not affected (Fig. 6 A). It was previously shown that the R28A mutant was not capable of rescuing the radiation sensitivity phenotype of NBS cells, whereas it did fully rescue the intra–S-phase checkpoint defect, at least at higher doses of irradiation (Lee et al., 2003). In contrast, primary B cells derived from a humanized mouse model in which another key amino acid at the phosphopeptide recognition interface of the NBS1 FHA domain had been mutated to Ala (H45A) showed partial G2/M and intra–S-phase checkpoint defects specifically at lower doses of irradiation (Difilippantonio et al., 2007). To test whether the R28A mutation causes a similar checkpoint defect, we measured alterations in the mitotic index in response to low (sublethal) doses of irradiation (1–3 Gy) in NBS fibroblasts stably transduced with full-length wild-type and R28A NBS1. Consistent with previous findings (Falck et al., 2005), NBS-iLB1 fibroblasts displayed a clear G2/M checkpoint defect in this dose range (Fig. 6 C). Stable transduction with wild-type NBS1 fully rescued the G2/M checkpoint arrest in response to 1–3 Gy of IR. However, stable

transduction with R28A mutant NBS1 only partially restored the G2/M checkpoint, which is similar to the situation in the mouse B cells expressing the H45A mutant (Fig. 6 C; Difilippantonio et al., 2007). Notably, this checkpoint defect was not caused by lower expression levels of the mutant transgene as compared with the wild type (Fig. 6 B). Collectively, these results suggest that the constitutive CK2-dependent association of the MRN complex with MDC1 plays an important role in eliciting a full cell cycle checkpoint arrest.

Discussion

Previously, we and others have shown that MDC1 mediates accumulation of the MRN complex at sites of DSBs (Goldberg et al., 2003; Stewart et al., 2003; Lukas et al., 2004; Stucki et al., 2005). We also presented evidence that MDC1 exists in a complex with MRN in extracts from undamaged cells and that an intact NBS1 FHA domain is essential for the stability of this interaction and for efficient retention of the MRN complex in γ-H2AX–containing damaged chromatin regions (Goldberg et al., 2003; Lukas et al., 2004; Stucki et al., 2005). However, the precise mechanism by which MDC1 regulates the MRN complex remained unknown.

In this study, we identify a region in MDC1 that is essential for efficient accumulation of the MRN complex at sites of DSBs. This region of MDC1 features a repeated acidic sequence motif (the SDT motif), and our data, in combination with the accompanying study by Melander et al. (see p. 213 of this issue) and several recently published large-scale phosphorylation site screens of the human and mouse proteome (Beausoleil et al., 2004; Olsen et al., 2006; Villen et al., 2007), suggest that at least a subset of the SDT motifs in MDC1 are constitutively phosphorylated by the acidophilic kinase CK2 on highly conserved Ser and Thr residues. Furthermore, we present unexpected evidence that the doubly phosphorylated SDT motifs regulate accumulation and retention of the MRN complex in the DSB-flanking chromatin compartment via a mechanism that involves direct interaction with the NBS1 N-terminal FHA domain. Finally, we show that CK2 is essential for NBS1 accumulation in damaged chromatin and that depletion of CK2 disrupts the MDC1–MRN complex in vivo. Thus, our data successfully integrate and explain two observations whose interrelation has previously not been appreciated: first, we provide a mechanistic explanation as to why MDC1 and the MRN complex exist in a complex even before DNA damage; and second, our findings also put into perspective the previous observation that an intact FHA domain of NBS1 is critical for efficient accumulation of the MRN complex at sites of DSBs (Kobayashi et al., 2002; Zhao et al., 2002; Cerosaletti and Concannon, 2003; Lee et al., 2003; Horejsi et al., 2004; Lukas et al., 2004) and for an intact DDR in living organisms (Difilippantonio et al., 2005, 2007).

However, it is essential to appreciate that not all MRN functions seem to require MDC1. For instance, DNA end processing activities of MRN do not appear to be dependent on MDC1 (Jazayeri et al., 2006). Furthermore, there are no indications that MRN's role in mediating ATM activation would require MDC1 (Lee and Paull, 2005). Finally, MRN seems to occupy two distinct compartments at sites of DSBs: it accumulates on single-stranded DNA regions generated by enzymatic resection of DSBs (Jazayeri et al., 2006) as well as in large chromatin domains flanking DSBs that often span several thousand base pairs (Bekker-Jensen et al., 2006). Although the accumulation of MRN on single-stranded DNA does not require MDC1 (Bekker-Jensen et al., 2006), accumulation and retention of MRN in γ-H2AX–containing chromatin are critically dependent on MDC1 (Goldberg et al., 2003; Stewart et al., 2003; Lukas et al., 2004; Stucki et al., 2005) and on CK2-dependent phosphorylation of its SDT repeats (Melander et al., 2008; this study).

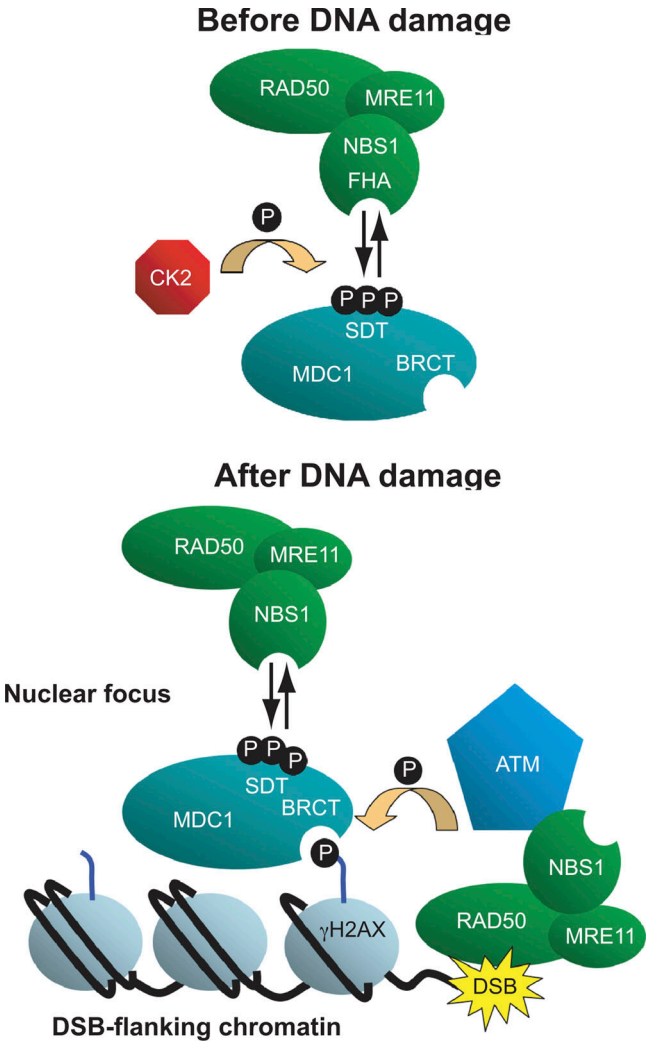

Figure 7. **Model of the mechanism of the MDC1–MRN interaction before and after DNA damage.** See Discussion for details.

Based on these novel findings and on previously published observations, we propose the following model of the events that occur before and after a cell has suffered genotoxic stress that generates DSBs (Fig. 7): in the absence of DNA damage, MDC1 is phosphorylated on multiple sites by CK2 and perhaps other constitutively active kinases. The MRN complex associates with MDC1 through direct interaction between the N-terminal FHA domain of the NBS1 subunit and the CK2-phosphorylated SDT repeat region of MDC1. Upon induction of DSBs in the genome, a fraction of MRN (that is probably not associated with MDC1) is rapidly deployed to the free DNA ends. Once bound to the

DNA, MRN participates in a multitude of events that include DNA end processing and tethering of DNA molecules that may facilitate accurate repair as well as activation of the ATM signaling cascade (for review see Williams et al., 2007). Although the precise mechanisms of these processes are still not understood in detail, there is no experimental indication that the MRN complex would require MDC1 for these functions. However, in a second step, after the ATM signaling cascade has been initiated, the MDC1-bound fraction of MRN enters the stage; once activated, ATM phosphorylates a vast variety of targets. Among these targets are H2AX molecules in nucleosomes that are located close to the break site. Phosphorylated H2AX is recognized by MDC1 through its C-terminal BRCT domains (Stucki et al., 2005). MDC1, along with the MDC1-bound fraction of MRN, forms a tight complex with phosphorylated H2AX, thus recruiting more MRN to the chromatin compartments flanking DSBs (Stucki et al., 2005; Lou et al., 2006). This process is manifested by the formation of microscopically discernible nuclear foci containing both MDC1 and the MRN complex.

Although such a model of MDC1–MRN interplay is intriguing, there are several outstanding issues that need to be discussed. It is clear that the interaction between MDC1 and the MRN complex is constitutive, but it is still dependent on the phosphorylation of MDC1 by CK2. A very similar mechanism has recently been described in two different aspects of the mammalian DDR, namely single-strand DNA break repair and DSB repair by nonhomologous end joining (Koch et al., 2004; Loizou et al., 2004). CK2 phosphorylates XRCC1, an adaptor protein that recruits several repair factors to single-stranded break sites (Loizou et al., 2004). In this case, the CK2 phosphorylation mark creates a binding site for the FHA domain–containing proteins polynucleotide kinase (PNK), aparataxin, and Xip1 (Loizou et al., 2004; Luo et al., 2004; Bekker-Jensen et al., 2007). In addition, PNK recruitment to sites of DSBs by XRCC4 is also mediated by the CK2-dependent phosphorylation of XRCC4 (Koch et al., 2004). Thus, the mechanisms of PNK, aparataxin, and Xip1 recruitment by XRCC1 and PNK recruitment by XRCC4 closely resemble MRN chromatin retention by MDC1. However, although the recruitment of PNK by XRCC1 was abolished by the CK2 inhibitor TBB (Loizou et al., 2004), we were unable to abolish NBS1 recruitment to damaged chromatin by using the same inhibitor and other (even more potent) small-molecule CK2 inhibitors. One possible explanation for this discrepancy may lie in the existence of one or more CK2-related acidophilic kinases that are capable of targeting the MDC1 SDT repeats. However, the fact that down-regulation of CK2 by siRNA completely abolishes NBS1 recruitment to damaged chromatin argues against this possibility but rather suggests that the CK2 inhibitors were not potent enough to reduce CK2 activity sufficiently to produce an effectual reduction in MDC1 phosphorylation. Indeed, in vivo phosphorylation analysis of MDC1 by Melander et al. (2008) reveals that treatment of cells with CK2 inhibitors maximally reduced SDT phosphorylation levels to 50%. This may not be enough for a visually discernible defect in NBS1 foci formation.

With the discovery of the mechanism by which MDC1 mediates accumulation and retention of the MRN complex in γ-H2AX–containing damaged chromatin regions, an important step in the hierarchy of events that lead to the formation of nuclear foci at sites of DSBs has been resolved. Although we do not yet understand the function of MRN in the DSB-flanking chromatin compartment, one intriguing possibility is that MDC1-bound MRN may act as a mediator of downstream phosphorylation events of the DDR. In this case, the MDC1–MRN complex may enhance the DSB-induced signal by means of a positive feedback loop: MDC1–MRN accumulates as the γ-H2AX mark spreads into more distal chromatin regions, thus helping to trigger a global DDR even in the presence of very low numbers of DSBs. Consistent with such a scenario is the observation that cells expressing NBS1 with a mutated FHA domain display a partial G2/M checkpoint defect at low doses of irradiation (Difilippantonio et al., 2007; this study), whereas the checkpoint seems to be normal at higher doses (Difilippantonio et al., 2007). This suggests that the prevalent role of the MDC1–MRN complex in checkpoint activation may not constitute the initiation of the signal but rather its amplification. The discovery of the SDT region of MDC1 and its specific role in MRN localization in response to DNA damage will greatly facilitate the investigation of functional aspects of MRN in the DSB-flanking chromatin compartment.

Materials and methods

Cell culture and gene transfer

$MDC1^{-/-}$ and $MDC1^{+/+}$ MEFs were gifts from J. Chen (Yale University, New Haven, CT). NBS-iLB1 cells stably transduced with wild-type NBS1 and R28A mutant NBS1 were gifts from S. Jackson (University of Cambridge, Cambridge, UK) and K. Cerosaletti (University of Washington, Seattle, WA), respectively. MEFs, HeLa, U2OS, and NBS-iLB1 cells were cultured in DME (Invitrogen) supplemented with 10% FCS. Transfection of plasmids was performed using either Lipofectamine 2000 (Invitrogen) or calcium phosphate. Sf9 cells were cultured in Grace's insect medium (Invitrogen) supplemented with 10% FCS. Recombinant MRE11, RAD50, and NBS1 baculoviruses were gifts from V. Bohr (National Institute on Aging, Baltimore, MD). The Bac-To-Bac Baculovirus Expression System (Invitrogen) was used to generate and amplify recombinant baculoviruses. All steps were performed according to the manufacturer's protocols. CK2 inhibitors TBB and DMAT were purchased from EMD. Irradiation of MEFs was performed in an x-ray cabinet (Faxitron) at 5–10 Gy/min.

Plasmids

The full-length mouse MDC1 cDNA was a gift from A. Nussenzweig (National Institutes of Health, Bethesda, MD) and was HA tagged at the C terminus by PCR and cloned into pcDNA3.1(+) mammalian expression vector (Invitrogen). Human MDC1-GST constructs were generated by PCR amplification of the human MDC1 cDNA followed by cloning into pGEX4T3 bacterial expression vector (GE Healthcare). Myc-NBS1 (Falck et al., 2005) was subcloned into pFastBac transfer vector (Invitrogen) to generate recombinant NBS1 baculoviruses. Deletion mutants were generated by a standard PCR-based method, and point mutations were introduced using the QuikChange Site-Directed Mutagenesis kit (Stratagene).

siRNA and transfections

The siRNA duplexes were 21 bp with a two-base deoxynucleotide overhang (Dharmacon Research). The sequences of the CK2α and CK2α′ siRNA oligonucleotides used were GAUGACUACCAGCUGGUUCdTdT and CAGUCUGAGGAGCCGCGAGdTdT, respectively. The control siRNA used was CGUACGCGGAAUACUUCGAdTdT. Cells were transfected with siRNA duplexes by using Oligofectamine (Invitrogen) according to the manufacturer's instructions. Cells were routinely harvested 72 h after siRNA transfection.

Cell extraction and protein purification

HeLa nuclear extract was purchased from Cilbiotech. Cell extraction for immunoblot analysis was described previously (Stewart et al., 2003).

MDC1-GST fragments were affinity purified on glutathione–Sepharose beads (GE Healthcare). Sf9 cells expressing recombinant MRN, MR, and N were lysed by sonication in buffer A (50 mM sodium phosphate, pH 7.0, 0.3 M NaCl, 10% glycerol, and 0.5 mM PMSF) containing 20 mM imidazol followed by centrifugation. The supernatants were loaded on Hi-Trap chelating (Ni^{2+}) columns (GE Healthcare) equilibrated with buffer A. The columns were washed with 50 ml buffer A/20 mM imidazol and with 50 ml buffer A/50 mM imidazol. Proteins were eluted with a 50-ml linear concentration gradient of 50–350 mM imidazole in buffer A. MRN-containing fractions were pooled and either used directly for analysis after dialysis against buffer B (20 mM Tris-HCl, pH 8.0, 150 mM NaCl, 10% glycerol, and 1 mM DTT) or loaded on 1-ml HiTrapQ columns (GE Healthcare) for further purification. The HiTrapQ columns were eluted with a 10-ml linear concentration gradient of 50–500 mM NaCl.

Antibodies and immunological techniques

Mouse monoclonal HA antibodies were purchased from Covance Research Products. The anti–mouse NBS1 antibody was a gift from A. Nussenzweig. The antibodies used against human Nbs1 were obtained from Genetex, Novus, and Millipore. Antibodies against phospho-Nbs1 Ser-343 and anti-phospho-H2AX were obtained from Genetex and Millipore, respectively. Anti-SMC1, phospho-SMC1 Ser-966, and H2AX antibodies were purchased from Bethyl, and the antiphospho-53BP1 and anti-53BP1 antibodies were obtained from Cell Signaling Technology. Sheep polyclonal antibodies against human MDC1, MRE11, and RAD50 have been described previously (Goldberg et al., 2003). Rabbit polyclonal antibodies to MDC1 have been described previously (Stewart et al., 2003). The anti-CK2α and -CK2α′ antibodies were purchased from Santa Cruz Biotechnology, Inc. Phosphospecific MDC1 antibodies were raised in rabbits to the MDC1 phosphopeptides GFIDS(P)DT(P)DA and TERDS(P)DT(P)DV and were affinity purified using the phosphorylated and nonphosphorylated peptides (Eurogentec).

For immunoprecipitation, HeLa cells were lysed for 30 min in NETN lysis buffer (50 mM Tris-HCl, pH 7.5, 150 mM NaCl, 1 mM EDTA, 2 mM $MgCl_2$, 1% NP-40 supplemented with protease inhibitors [Roche], and benzonase [EMD]). The clarified extract was precleared with the appropriate IgG (Dako) and protein A or G beads (GE Healthcare) for 1 h at 4°C. 5 µg of immunoprecipitating antibody was added with protein A or G beads to the precleared supernatant and incubated for 3 h at 4°C. The immunocomplexes were washed four times in NETN lysis buffer (containing 0.5% NP-40), boiled in SDS sample buffer, and loaded on an SDS-polyacrylamide gel. Proteins were analyzed by immunoblotting using standard methods.

For immunofluorescence staining, cells were grown on glass coverslips, fixed in ice-cold methanol, and stained with the indicated antibodies for 1 h at room temperature. Secondary antibodies were purchased from Jackson ImmunoResearch Laboratories (FITC and rhodamine) and Invitrogen (AlexaFluor488 and -596). Images were captured at room temperature on a confocal microscope (SP2; Leica) with a 40× NA 1.25 oil immersion objective (Leica; Figs. 1, 4, and 6) and on a microscope (Eclipse E600; Nikon) with a 60× oil immersion objective (Nikon; Fig. 5).

Biochemical analysis

For GST pull-down assays, purified 5 µg GST fusion proteins were mixed with 200 µg HeLa nuclear extract or with 5 µg of purified MRN. Where indicated, GST fusion proteins were pretreated with 100 U CK2 (New England BioLabs, Inc.). The mixture was incubated at 4°C for 30 min to allow binding. Glutathione–Sepharose beads were then added, and the suspension was incubated at 4°C for a further 60 min. The beads were washed three times with wash buffer (50 mM Tris, pH 7.5, 120 mM NaCl, 1 mM DTT, and 0.2% NP-40), resuspended in SDS loading buffer, and analyzed by SDS-PAGE and immunoblotting. For peptide pull-down analysis, the biotinylated synthetic peptide Btn-NH-SGSFIDSD[pT]DAEEERI-COOH (Eurogentec) was used. Where indicated, 25 nmol of the peptide was incubated with 500 U of recombinant CK2 (New England Biolabs, Inc.) at 30°C for 45 min and with 100 U λ phosphatase (New England Biolabs, Inc.) at 30°C for 20 min. Peptide pull-down analysis was performed as described previously (Stucki et al., 2005).

CK2 in vitro kinase assays for phosphorylation site mapping was performed by adding 100 ng of recombinant CK2α (Millipore) to 1 µg GST-MDC1 (amino acids 141–621) in CK2 kinase buffer (20 mM MOPS, pH 7.2, 25 mM β-glycerophosphate, 5 mM EGTA, 1 mM sodium orthovanadate, 37.5 mM $MgCl_2$, 1 mM DTT, 100 µM ATP, and 10 µCi γ-[^{32}P]ATP) and incubating for 10 min at 30°C. Kinase reactions were inactivated by boiling in SDS sample buffer and were run on an SDS-polyacrylamide gel. Gels were stained with Coomassie blue and either dried and subjected to autoradiography, or the GST-MDC1 band was excised and processed for mass spectrometric phospho–amino acid analysis (Jowsey et al., 2007). Mutation of putative CK2 phosphorylation sites in the GST-MDC1 fragment was performed using site-directed mutagenesis (Stratagene).

Checkpoint analysis

G2/M checkpoint analysis was performed as described previously (Falck et al., 2005). In brief, cells were irradiated with the indicated doses during the exponential growth phase. 1 h later, cells were harvested, fixed with 70% ethanol/PBS, and incubated overnight at −20°C. Fixed cells were washed with PBS and permeabilized with 0.25% Triton X-100/PBS on ice for 10 min. Cells were stained with an antiphosphohistone H3 antibody (Millipore) and propidium iodide. Data were acquired with a flow cytometer (FC500; Becton Dickinson).

Phosphorylation site analysis by mass spectrometry

MDC1 samples that had been incubated with CK2 with or without ATP were subjected to electrophoresis on a 4–12% polyacrylamide gel that was stained with colloidal Coomassie blue. MDC1 bands were excised from the gel, washed with 0.1% NH_4HCO_3 and 50% acetonitrile/50 mM NH_4HCO_3, reduced with 10 mM DTT in 0.1 M NH_4HCO_3 for 45 min at 65°C, and alkylated by the addition of 50 mM iodoacetamide for 30 min at room temperature. Gel pieces were then washed in 0.1% NH_4HCO_3 and 50% acetonitrile/50 mM NH_4HCO_3, dried, and incubated with 25 mM triethylammonium bicarbonate with 5 µg/ml trypsin for 16 h at 30°C. For identification of phosphorylation sites, the extracted tryptic peptides were analyzed by liquid chromatography mass spectrometry on a spectrometer (4000 Q-TRAP; Applied Biosystems) with precursor ion scanning as described previously (Williamson et al., 2006). The tandem mass spectrometry spectra were searched against a local database containing the GST-MDC1 sequence using the Mascot search algorithm (www.matrixscience.com) run on a local server. Sites of phosphorylation were validated by manual inspection of the mass spectrometry spectra using Analyst 1.4.1 software (MDS Sciex).

Online supplemental material

Fig. S1 shows a sequence alignement of the SDT repeats in human, mouse, zebrafish, and honey bee MDC1. Fig. S2 shows the purified MDC1–MRN complex isolated from HeLa nuclear extract. Online supplemental material is available at http://www.jcb.org/cgi/content/full/jcb.200709008/DC1.

We thank Jiri Lukas for stimulating discussions and for communicating unpublished results, Steve Jackson for communicating unpublished results, and Junjie Chen, André Nussenzweig, Karen Cerosaletti, Vilhelm Bohr, Graeme Smith, and Steve Jackson for providing valuable reagents. Stéphanie Jungmichel is acknowledged for comments and critical reading of the manuscript.

This work was supported by grants from the Swiss National Foundation (grant 3100A0-111818), the UBS AG (Im Auftrag eines Kunden), and by the Kanton of Zürich. G.S. Stewart, E.S. Miller, and K. Townsend are supported by Cancer Research UK Career Development fellowships (ref: C17183/A5592).

Submitted: 4 September 2007
Accepted: 19 March 2008

References

Beausoleil, S.A., M. Jedrychowski, D. Schwartz, J.E. Elias, J. Villen, J. Li, M.A. Cohn, L.C. Cantley, and S.P. Gygi. 2004. Large-scale characterization of HeLa cell nuclear phosphoproteins. *Proc. Natl. Acad. Sci. USA.* 101:12130–12135.

Bekker-Jensen, S., C. Lukas, R. Kitagawa, F. Melander, M.B. Kastan, J. Bartek, and J. Lukas. 2006. Spatial organization of the mammalian genome surveillance machinery in response to DNA strand breaks. *J. Cell Biol.* 173:195–206.

Bekker-Jensen, S., K. Fugger, J.R. Danielsen, I. Gromova, M. Sehested, J. Celis, J. Bartek, J. Lukas, and N. Mailand. 2007. Human Xip1 (C2orf13) is a novel regulator of cellular responses to DNA strand breaks. *J. Biol. Chem.* 282:19638–19643.

Bhaskara, V., A. Dupre, B. Lengsfeld, B.B. Hopkins, A. Chan, J.H. Lee, X. Zhang, J. Gautier, V. Zakian, and T.T. Paull. 2007. Rad50 adenylate kinase activity regulates DNA tethering by Mre11/Rad50 complexes. *Mol. Cell.* 25:647–661.

Burma, S., B.P. Chen, M. Murphy, A. Kurimasa, and D.J. Chen. 2001. ATM phosphorylates histone H2AX in response to DNA double-strand breaks. *J. Biol. Chem.* 276:42462–42467.

Celeste, A., O. Fernandez-Capetillo, M.J. Kruhlak, D.R. Pilch, D.W. Staudt, A. Lee, R.F. Bonner, W.M. Bonner, and A. Nussenzweig. 2003. Histone H2AX phosphorylation is dispensable for the initial recognition of DNA breaks. *Nat. Cell Biol.* 5:675–679.

Cerosaletti, K.M., and P. Concannon. 2003. Nibrin forkhead-associated domain and breast cancer C-terminal domain are both required for nuclear focus formation and phosphorylation. *J. Biol. Chem.* 278:21944–21951.

Costanzo, V., T. Paull, M. Gottesman, and J. Gautier. 2004. Mre11 assembles linear DNA fragments into DNA damage signaling complexes. *PLoS Biol.* 2:E110.

D'Amours, D., and S.P. Jackson. 2002. The Mre11 complex: at the crossroads of DNA repair and checkpoint signalling. *Nat. Rev. Mol. Cell Biol.* 3:317–327.

Difilippantonio, S., A. Celeste, O. Fernandez-Capetillo, H.T. Chen, B. Reina San Martin, F. Van Laethem, Y.P. Yang, G.V. Petukhova, M. Eckhaus, L. Feigenbaum, et al. 2005. Role of Nbs1 in the activation of the Atm kinase revealed in humanized mouse models. *Nat. Cell Biol.* 7:675–685.

Difilippantonio, S., A. Celeste, M.J. Kruhlak, Y. Lee, M.J. Difilippantonio, L. Feigenbaum, S.P. Jackson, P.J. McKinnon, and A. Nussenzweig. 2007. Distinct domains in Nbs1 regulate irradiation-induced checkpoints and apoptosis. *J. Exp. Med.* 204:1003–1011.

Durocher, D., and S.P. Jackson. 2002. The FHA domain. *FEBS Lett.* 513:58–66.

Falck, J., J. Coates, and S.P. Jackson. 2005. Conserved modes of recruitment of ATM, ATR and DNA-PKcs to sites of DNA damage. *Nature.* 434:605–611.

Fernandez-Capetillo, O., A. Lee, M. Nussenzweig, and A. Nussenzweig. 2004. H2AX: the histone guardian of the genome. *DNA Repair (Amst.).* 3:959–967.

Glover, J.N., R.S. Williams, and M.S. Lee. 2004. Interactions between BRCT repeats and phosphoproteins: tangled up in two. *Trends Biochem. Sci.* 29:579–585.

Goldberg, M., M. Stucki, J. Falck, D. D'Amours, D. Rahman, D. Pappin, J. Bartek, and S.P. Jackson. 2003. MDC1 is required for the intra-S-phase DNA damage checkpoint. *Nature.* 421:952–956.

Horejsi, Z., J. Falck, C.J. Bakkenist, M.B. Kastan, J. Lukas, and J. Bartek. 2004. Distinct functional domains of Nbs1 modulate the timing and magnitude of ATM activation after low doses of ionizing radiation. *Oncogene.* 23:3122–3127.

Jazayeri, A., J. Falck, C. Lukas, J. Bartek, G.C. Smith, J. Lukas, and S.P. Jackson. 2006. ATM- and cell cycle-dependent regulation of ATR in response to DNA double-strand breaks. *Nat. Cell Biol.* 8:37–45.

Jowsey, P., N.A. Morrice, C.J. Hastie, H. McLauchlan, R. Toth, and J. Rouse. 2007. Characterisation of the sites of DNA damage-induced 53BP1 phosphorylation catalysed by ATM and ATR. *DNA Repair (Amst.).* 6:1536–1544.

Kobayashi, J., H. Tauchi, S. Sakamoto, A. Nakamura, K. Morishima, S. Matsuura, T. Kobayashi, K. Tamai, K. Tanimoto, and K. Komatsu. 2002. NBS1 localizes to gamma-H2AX foci through interaction with the FHA/BRCT domain. *Curr. Biol.* 12:1846–1851.

Koch, C.A., R. Agyei, S. Galicia, P. Metalnikov, P. O'Donnell, A. Starostine, M. Weinfeld, and D. Durocher. 2004. Xrcc4 physically links DNA end processing by polynucleotide kinase to DNA ligation by DNA ligase IV. *EMBO J.* 23:3874–3885.

Lee, J.H., and T.T. Paull. 2005. ATM activation by DNA double-strand breaks through the Mre11-Rad50-Nbs1 complex. *Science.* 308:551–554.

Lee, J.H., B. Xu, C.H. Lee, J.Y. Ahn, M.S. Song, H. Lee, C.E. Canman, J.S. Lee, M.B. Kastan, and D.S. Lim. 2003. Distinct functions of Nijmegen breakage syndrome in ataxia telangiectasia mutated-dependent responses to DNA damage. *Mol. Cancer Res.* 1:674–681.

Loizou, J.I., S.F. El-Khamisy, A. Zlatanou, D.J. Moore, D.W. Chan, J. Qin, S. Sarno, F. Meggio, L.A. Pinna, and K.W. Caldecott. 2004. The protein kinase CK2 facilitates repair of chromosomal DNA single-strand breaks. *Cell.* 117:17–28.

Lou, Z., K. Minter-Dykhouse, S. Franco, M. Gostissa, M.A. Rivera, A. Celeste, J.P. Manis, J. van Deursen, A. Nussenzweig, T.T. Paull, et al. 2006. MDC1 maintains genomic stability by participating in the amplification of ATM-dependent DNA damage signals. *Mol. Cell.* 21:187–200.

Lukas, C., F. Melander, M. Stucki, J. Falck, S. Bekker-Jensen, M. Goldberg, Y. Lerenthal, S.P. Jackson, J. Bartek, and J. Lukas. 2004. Mdc1 couples DNA double-strand break recognition by Nbs1 with its H2AX-dependent chromatin retention. *EMBO J.* 23:2674–2683.

Luo, H., D.W. Chan, T. Yang, M. Rodriguez, B.P. Chen, M. Leng, J.J. Mu, D. Chen, Z. Songyang, Y. Wang, and J. Qin. 2004. A new XRCC1-containing complex and its role in cellular survival of methyl methanesulfonate treatment. *Mol. Cell. Biol.* 24:8356–8365.

Maser, R.S., K.J. Monsen, B.E. Nelms, and J.H. Petrini. 1997. hMre11 and hRad50 nuclear foci are induced during the normal cellular response to DNA double-strand breaks. *Mol. Cell. Biol.* 17:6087–6096.

Matsuoka, S., B.A. Ballif, A. Smogorzewska, E.R. McDonald III, K.E. Hurov, J. Luo, C.E. Bakalarski, Z. Zhao, N. Solimini, Y. Lerenthal, et al. 2007. ATM and ATR substrate analysis reveals extensive protein networks responsive to DNA damage. *Science.* 316:1160–1166.

Melander, F., S. Bekker-Jensen, J. Falck, J. Bartek, N. Mailand, and J. Lukas. 2008. Phosphorylation of SDT repeats in the MDC1 N terminus triggers retention of NBS1 at the DNA damage–modified chromatin. *J. Cell Biol.* 181:213–226.

Olsen, J.V., B. Blagoev, F. Gnad, B. Macek, C. Kumar, P. Mortensen, and M. Mann. 2006. Global, in vivo, and site-specific phosphorylation dynamics in signaling networks. *Cell.* 127:635–648.

Stewart, G.S., B. Wang, C.R. Bignell, A.M.R. Taylor, and S.J. Elledge. 2003. MDC1 is a mediator of the mammalian DNA damage checkpoint. *Nature.* 421:961–966.

Stracker, T.H., J.W. Theunissen, M. Morales, and J.H. Petrini. 2004. The Mre11 complex and the metabolism of chromosome breaks: the importance of communicating and holding things together. *DNA Repair (Amst.).* 3:845–854.

Stracker, T.H., M. Morales, S.S. Couto, H. Hussein, and J.H. Petrini. 2007. The carboxy terminus of NBS1 is required for induction of apoptosis by the MRE11 complex. *Nature.* 447:218–221.

Stucki, M., and S.P. Jackson. 2004. MDC1/NFBD1: a key regulator of the DNA damage response in higher eukaryotes. *DNA Repair (Amst.).* 3:953–957.

Stucki, M., and S.P. Jackson. 2006. gammaH2AX and MDC1: anchoring the DNA-damage-response machinery to broken chromosomes. *DNA Repair (Amst.).* 5:534–543.

Stucki, M., J.A. Clapperton, D. Mohammad, M.B. Yaffe, S.J. Smerdon, and S.P. Jackson. 2005. MDC1 directly binds phosphorylated histone H2AX to regulate cellular responses to DNA double-strand breaks. *Cell.* 123:1213–1226.

Villen, J., S.A. Beausoleil, S.A. Gerber, and S.P. Gygi. 2007. Large-scale phosphorylation analysis of mouse liver. *Proc. Natl. Acad. Sci. USA.* 104:1488–1493.

Williams, R.S., J.S. Williams, and J.A. Tainer. 2007. Mre11-Rad50-Nbs1 is a keystone complex connecting DNA repair machinery, double-strand break signaling, and the chromatin template. *Biochem. Cell Biol.* 85:509–520.

Williamson, B.L., J. Marchese, and N. Morrice. 2006. Automated identification and quantification of protein phosphorylation sites by LC/MS on a hybrid triple quadrupole linear ion trap mass spectrometer. *Mol. Cell. Proteomics.* 5:337–346.

Yaffe, M.B., G.G. Leparc, J. Lai, T. Obata, S. Volinia, and L.C. Cantley. 2001. A motif-based profile scanning approach for genome-wide prediction of signaling pathways. *Nat. Biotechnol.* 19:348–353.

Zhao, S., W. Renthal, and E.Y. Lee. 2002. Functional analysis of FHA and BRCT domains of NBS1 in chromatin association and DNA damage responses. *Nucleic Acids Res.* 30:4815–4822.

Zhou, B.B., and S.J. Elledge. 2000. The DNA damage response: putting checkpoints in perspective. *Nature.* 408:433–439.